Journal of Colloid and Interface Science 369 (2012) 274–286

Contents lists available at SciVerse ScienceDirect

Journal of Colloid and Interface Science

www.elsevier.com/locate/jcis

Solubility limits and phase diagrams for fatty acids in anionic (SLES) and zwitterionic (CAPB) micellar surfactant solutions

Sylvia S. Tzocheva [a], Peter A. Kralchevsky [a,*], Krassimir D. Danov [a], Gergana S. Georgieva [a], Albert J. Post [b], Kavssery P. Ananthapadmanabhan [b]

[a] Department of Chemical Engineering, Faculty of Chemistry, Sofia University, 1164 Sofia, Bulgaria
[b] Unilever Research and Development, Trumbull, CT 06611, USA

ARTICLE INFO

Article history:
Received 17 October 2011
Accepted 12 December 2011
Available online 22 December 2011

Keywords:
Solubility limit of fatty acids
Fatty acids in surfactant micelles
Solubilization energy
CMC for mixed micelles
Regular solution theory

ABSTRACT

The limiting solubility of fatty acids in micellar solutions of the anionic surfactant sodium laurylethersulfate (SLES) and the zwitterionic surfactant cocamidopropyl betaine (CAPB) is experimentally determined. Saturated straight-chain fatty acids with $n = 10$, 12, 14, 16, and 18 carbon atoms were investigated at working temperatures of 25, 30, 35, and 40 °C. The rise of the fatty acid molar fraction in the micelles is accompanied by an increase in the equilibrium concentration of acid monomers in the aqueous phase. Theoretically, the solubility limit is explained with the precipitation of fatty acid crystallites when the monomer concentration reaches the solubility limit of the acid in pure water. In agreement with theory, the experiment shows that the solubility limit is proportional to the surfactant concentration. For ideal mixtures, the plot of the log of solubility limit vs. the chainlength, n, must be a straight line, which is fulfilled for $n = 14$, 16, and 18. For the fatty acids of shorter chains, $n = 10$ and 12, a deviation from linearity is observed, which is interpreted as non-ideal mixing due to a mismatch between the chainlengths of the surfactant and acid. The data analysis yields the solubilization energy and the interaction parameter for the fatty acid molecules in surfactant micelles. By using the determined parameter values, phase diagrams of the investigated mixed solutions are constructed. The four inter-domain boundary lines intersect in a quadruple point, whose coordinates have been determined. The results can be applied for the interpretation and prediction of the solubility, and phase behavior of medium- and long-chain fatty acids and other amphiphiles that are solubilizable in micellar surfactant solutions, as well as for determining the critical micellization concentration (CMC) of the respective mixed solution.

1. Introduction

At room temperature, the protonated fatty (carboxylic, alkanoic) acids with $n \geqslant 12$ carbon atoms have a very low molecular solubility in water. However, they can be dissolved (solubilized) in micellar solutions of conventional surfactants. In such solutions, the predominant part of the fatty acid is incorporated in the formed mixed micelles. The latter can serve as carriers of fatty acid molecules during the processes of adsorption and formation of disperse systems (foams, emulsions, and suspensions). The adsorption or solubilization of fatty acids can essentially influence the interfacial properties, as well as the stability and rheology of dispersions.

An important example represents the foam generated from surfactant solutions that contain solubilized fatty acid. The micelles provide fatty acid molecules to the surface of the newly formed bubbles in the foam, where they form dense and elastic (rather than fluid) adsorption monolayers. This fact has at least two consequences. First, the immobilization of the air/water interface by the amphiphile of low water solubility slows down the film and foam drainage [1–4]. Second, the produced bubbles are considerably smaller and the foam viscoelasticity is markedly enhanced, which is important for the properties of many consumer products [5–7]. Such effects have been observed with additives as dodecanol [4,8–10], lauric and myristic acids [11–13], as well as with sodium and potassium salts of the fatty acids [11,14]. They affect the bubble surface mobility, foam drainage, and rheology [15]. The aqueous solutions of sodium and potassium carboxylates always contain molecules of the respective carboxylic acid, which are produced by spontaneous protonation of the carboxylate anion [16–20]. The equilibrium and dynamics of dissolution of calcium salts of the long-chain fatty acids have been also investigated [21,22].

The solubility of a given fatty acid in micellar surfactant solutions is limited. Above a certain concentration, precipitate of fatty acid crystallites appears in the solution. This concentration is usually termed "solubility limit" or "saturation concentration". Fatty acid precipitation can be observed even upon dilution of an initially clear solution containing mixed micelles. Indeed, upon

* Corresponding author. Fax: +359 2 962 5643.
E-mail address: pk@lcpe.uni-sofia.bg (P.A. Kralchevsky).

0021-9797/$ - see front matter © 2011 Elsevier Inc. All rights reserved.
doi:10.1016/j.jcis.2011.12.036

dilution, the micelles release mostly monomers of the water-soluble conventional surfactant, whereas the molar fraction of the fatty acid in the micelles increases. At a certain degree of dilution, this leads to the precipitation of fatty acid crystallites.

Our goal in the present study is to clarify the physicochemical reason for the existence of a solubility limit for medium- and long-chain fatty acids in micellar surfactant solutions and to give a quantitative description of the related phenomena. This includes investigation of the dependence of the solubility limit on the concentration of conventional surfactant (Section 3) and determination of the solubilization energy of fatty acid molecules in the surfactant micelles. The theory of regular solutions is used to quantitatively describe the interactions between the components in the mixed micelles. For the investigated systems, the conventional approach by Rubingh [23] is inapplicable to determine the interaction parameter (see below). For this reason, a completely new approach was developed, which is based on the analysis of the dependence of saturation concentration on the fatty acid chain-length (Section 4). Original phase diagrams are constructed, which visualize the phase behavior of the system at concentrations below the liquid crystal region. The phase domains correspond to: (i) solutions with mixed micelles; (ii) solutions with coexistent micelles and crystallites; (iii) solutions that contain only crystallites but no micelles, and (iv) molecular solutions that contain only monomers, without micelles and crystallites. Such a diagram includes also the dependence of the critical micellization concentration of the mixed solutions (CMC_M) on the solution's composition. The boundaries between the phase domains are theoretically predicted using the determined thermodynamic parameters of the system and verified in additional experiments (Section 5). The results could be of interest for any applications, in which mixed micellar solutions of conventional surfactants and fatty acids are used.

2. Materials and methods

The following straight-chain saturated fatty acids were used: capric (decanoic) acid, ⩾99 %, from Alfa Aesar; lauric (dodecanoic) acid, ⩾99.5 % from Acros Organics; myristic (tetradecanoic) acid, ⩾98%, from Fluka; palmitic (hexadecanoic) acid, >98%, from Riedel-de-Haën, and stearic (octadecanoic) acid, 90–95%, from Fluka. For brevity, in the text, these fatty acids are denoted by HC_n at n = 10–18. All chemicals were used as received, without additional purification.

The anionic surfactant was sodium laurylethersulfate (SLES) with one ethylene oxide group, product of Stepan Co.; commercial name STEOL CS-170; molecular mass 332.4 g/mol. The critical micellization concentration of SLES is $CMC_S = 7 \times 10^{-4}$ M determined by both surface tension and conductivity measurements at 25 °C.

The zwitterionic surfactant with a quaternary ammonium cation was cocamidopropyl betaine (CAPB), product of Goldschmidt GmbH; commercial name Tego® Betain F50; molecular mass 356 g/mol. CAPB finds a wide application in personal-care detergency. The critical micellization concentration of CAPB is $CMC_S = 9 \times 10^{-5}$ M determined by surface tension measurements at 25 °C. CAPB is a derivate of coconut oil and contains admixtures of non-reacted coco fatty acids. The used batch sample containing 40 wt% CAPB was investigated by titration with NaOH and gas chromatography, and it was found that it contains 2.81 wt% coco fatty acids. In particular, a 100 mM CAPB solution contains 1.48 mM HC_8; 1.08 mM HC_{10}; 6.65 mM HC_{12}; 1.98 mM HC_{14}; 0.83 mM HC_{16}; and 0.37 mM HC_{18}; total 12.4 mM coco fatty acid. The latter background concentrations have been taken into account when determining the solubility limits of the respective fatty acids in micellar CAPB solutions.

The solutions were prepared with deionized water (Milli-Q purification system, Millipore, USA) of specific resistivity 18.2 M cm. The working procedure was as follows. First, the fatty acid was added to the micellar surfactant solution. Then, the solution was heated at 65 °C and stirred for 15 min. Next, it was placed in a thermostat, where it was kept for at least 24 h to equilibrate at the working temperature: 25, 30, 35, or 40 °C. The experiments were carried out at the natural pH of the prepared solutions, which slightly varies depending on the composition; see Appendix A for details.

The absorbance of light by the solutions was measured by a Unicam UV/VIS spectrophotometer (Unicam Ltd., Cambridge, UK) at wavelength λ = 500 nm. By definition, the absorbance is $A_\lambda = \log_{10}(I_0/I)$, where I_0 and I are the intensities of the incident and transmitted beams. The turbidity is due to light scattering by fatty acid crystallites or droplets. The aim of these measurements was to determine the solubility limit of the fatty acid in the micelles, which is detected as an abrupt increase of the solution's turbidity due to the appearance of crystallites. Before each absorbance measurement, the flask with the solution was shaken to disperse the sedimented crystallites, if any. From the obtained data, we determined the solubilization constant of each fatty acid in the surfactant micelles at the respective temperature, as explained in Section 4.4.

3. Experimental results

3.1. Data for the solubility limit

Typical experimental curves for the light absorbance vs. the concentration of fatty acid in micellar solutions are shown in Fig. 1a for SLES and in Fig. 1b for CAPB (100 mM surfactant concentration at 25 °C). In each separate curve, an abrupt increase in the absorbance is observed above a certain saturation concentration, which is denoted by $c_{A,sat}$ and indicates the appearance of fatty acid crystallites in the solution. In the case of capric acid (HC_{10}), at 35 and 40 °C, the turbidity is due to the appearance of droplets, instead of crystallites. {The melting temperature of HC_{10} is 31.5 °C [24].}

The general tendency is $c_{A,sat}$ to decrease with the increase of the number of carbon atoms, n, in the fatty acid molecule HC_n (Fig. 1). In other words, the solubility of HC_n in the micelles of SLES and CAPB decreases with the increase of the fatty acid chainlength. The only exclusion is observed with HC_{10}, which has a lower solubility than HC_{12} in CAPB solutions (Fig. 1b). The latter can be explained with a mismatch of the chainlengths of HC_{10} and CAPB, which leads to a less favorable mixing of the two components in the micelles (see below).

The experimental values of $c_{A,sat}$ for 100 mM surfactant solutions are given in Table 1 for SLES and CAPB. The molar fraction of the fatty acid in the mixed micelles is calculated from the expression:

$$y_{A,sat} = \frac{c_{A,sat}}{c_S + c_{A,sat}} \quad (1)$$

where c_S is the total input concentration of surfactant (e.g., SLES) in the solution; $c_{A,sat}$ is the total input concentration of fatty acid in the solution at saturation (at the solubility limit). In Eq. (1), we neglect the amount of surfactant and fatty acid in *monomeric* form, because our measurements of $c_{A,sat}$ are carried out at concentrations much above the CMC, so that the predominant part of the amphiphilic molecules are present in micellar form. In the case of CAPB, c_S includes also the concentrations of background coco fatty acids (admixtures in CAPB; see section 2) that are different from the investigated fatty acid, component A.

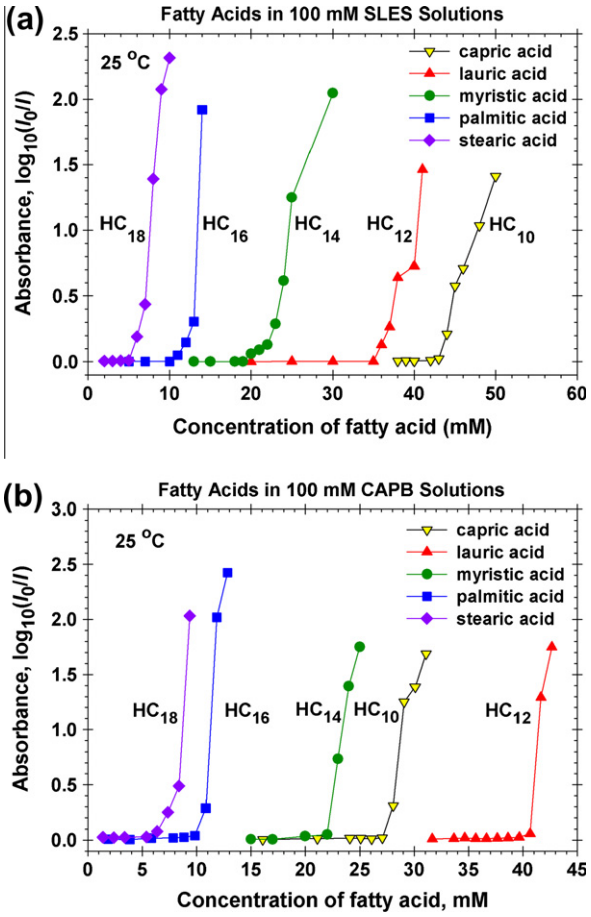

Fig. 1. Absorbance of light vs. the fatty acid concentration, c_A, for five acids at $T = 25$ °C. The surfactant solution is (a) 100 mM SLES and (b) 100 mM CAPB. The lines are guides to the eye.

3.2. Temperature dependence of the solubility limit

The temperature dependence of the solubility limit of fatty acids in micellar surfactant solutions is visualized in Fig. 2 in the form of plots of $y_{A,sat}$ vs. T for all investigated solutions. The strongest temperature dependence is observed with HC_{16} and HC_{18} in CAPB solutions. For all other systems, the dependence of $y_{A,sat}$ on temperature is relatively weak. For the CAPB solutions, the values of $y_{A,sat}$ corresponding to different acids become closer at 40 °C (Fig. 2b), whereas such tendency is absent in the case of SLES solutions (Fig. 2a). At all investigated temperatures, the general trend is $y_{A,sat}$ to decrease with the increase of the fatty acid chain-length, the only exclusion being HC_{10} in CAPB solutions.

3.3. Fatty acid saturation concentration vs. surfactant concentration

The dependence of the fatty acid saturation concentration, $c_{A,sat}$, on the surfactant concentration, c_S, was experimentally investigated. The obtained data (Fig. 3) indicate that $c_{A,sat}$ is proportional to c_S, viz.

$$c_{A,sat} = A_{sat} c_S \quad \text{where} \quad A_{sat} \equiv \frac{y_{A,sat}}{1 - y_{A,sat}} = \text{const.} \tag{2}$$

The above relation between A_{sat} and $y_{A,sat}$ follows from Eq. (1). The values of the coefficient A_{sat} determined from the slopes of the linear regressions in Fig. 3 are given in Table 2. As seen in this table, at 25 °C, the values of A_{sat} are close for the CAPB and SLES solutions and grow with the decrease of n. Exclusion is the result for capric acid, HC_{10}, in CAPB solutions. In view of Eq. (2), the data in Fig. 3 indicate that $y_{A,sat}$ is independent of the surfactant concentration, c_S, which is in agreement with the theoretical predictions (see Section 4.2). In other words, having determined $y_{A,sat}$ at a given surfactant concentration, e.g., at 100 mM as in Table 1, we can use the obtained $y_{A,sat}$ values for any other c_S.

4. Interpretation of the experimental data

4.1. Theoretical background

Here, we summarize the basic equations that will be subsequently used to interpret the solubility limit and to construct phase diagrams. In thermodynamics of mixed micelles, three kinds of mole fractions can be distinguished [25]: x_i – mole fraction of component i dissolved in monomeric form; y_i – mole fraction of component i in the micelles (in the micellar pseudophase), and z_i – total mole fraction of component i contained in the solution. All these molar fractions refer to the blend of amphiphilic molecules (the water is excluded). The input mole fraction z_i is fixed by the experimentalist when preparing the solution. The monomeric and micellar mole fractions, x_i and y_i, can be calculated from the mass-balance equations and the conditions for chemical equilibrium between micelles and monomers. The surfactant mass balance reads [25]:

$$z_i C_T = (C_T - CMC_M) y_i + x_i CMC_M \tag{3}$$

Here, C_T is the total concentration of (all kinds of) surfactant contained in the solution; CMC_M is the critical micellization concentration of the *mixed* surfactant solution. In addition, the chemical

Table 1
Experimental solubility limits for fatty acids in 100 mM surfactant (SLES or CAPB) solutions: Data for $c_{A,sat}$ and $y_{A,sat}$ vs. n at different temperatures.

n	25 °C		30 °C		35 °C		40 °C	
	$c_{A,sat}$ (mM)	$y_{A,sat}$	$c_{A,sat}$ (mM)	$y_{A,sat}$	$c_{A,sat}$ (mM)	$y_{A,sat}$	$c_{A,sat}$ (mM)	$y_{A,sat}$
SLES								
10	43	0.301	43	0.301	45	0.310	46	0.315
12	35	0.259	34	0.254	35	0.259	36	0.265
14	19	0.160	26	0.206	33	0.248	33	0.248
16	10	0.0909	12	0.107	15	0.130	15	0.130
18	5	0.0476	6	0.0566	8	0.0741	8	0.0741
CAPB								
10	27.1	0.196	25.6	0.187	25.1	0.184	25.1	0.184
12	40.7	0.278	33.7	0.241	33.7	0.241	33.7	0.241
14	22	0.166	28	0.202	28	0.202	28	0.202
16	9.8	0.0810	16.8	0.131	20.8	0.157	23.8	0.176
18	5.4	0.0457	11.4	0.0921	15.4	0.121	20.9	0.157

n Is the number of carbon atoms in the fatty acid molecule; $y_{A,sat}$ is the molar fraction of the fatty acid in the mixed micelles at saturation.

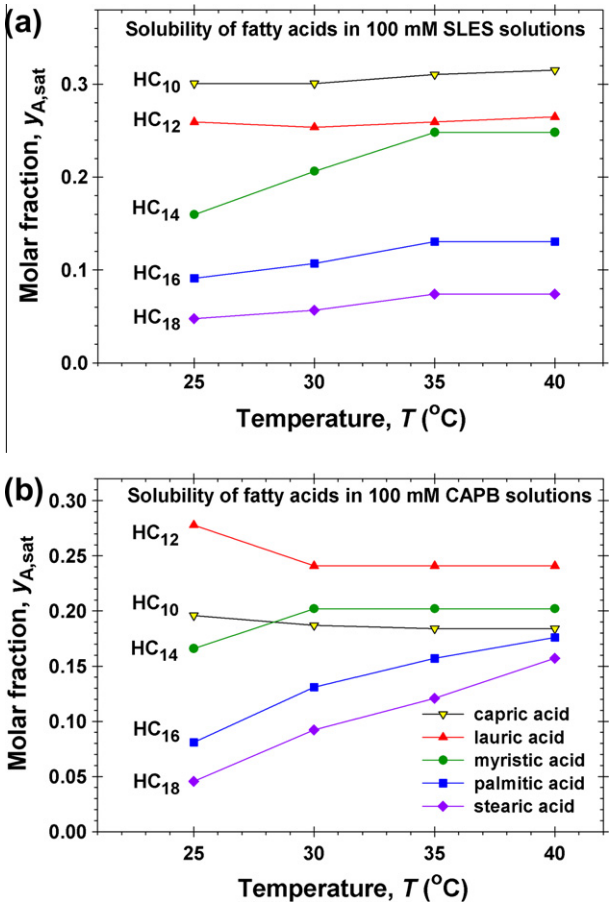

Fig. 2. Temperature dependence of the solubility of fatty acids in micellar surfactant solutions: Plot of the acid molar fraction at saturation, $y_{A,sat}$, vs. temperature, T, for five straight-chain saturated fatty acids. The surfactant solution is (a) 100 mM SLES, and (b) 100 mM CAPB. The lines are guides to the eye.

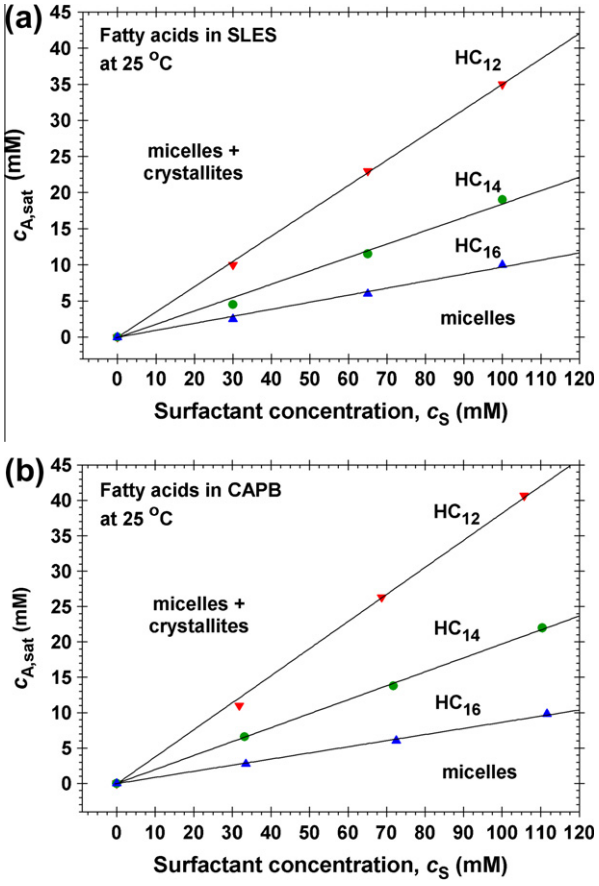

Fig. 3. Plot of the fatty acid concentration at saturation, $c_{A,sat}$, vs. the surfactant concentration, c_S for lauric (HC_{12}), myristic (HC_{14}) and palmitic (HC_{16}) acids. The surfactant is (a) SLES; (b) CAPB.

equilibrium between micelles and monomers with respect to the exchange of component i (Fig. 4) yields:

$$\mu^0_{i,\mathrm{mon}} + kT\ln(x_i\mathrm{CMC_M}) = \mu^0_{i,\mathrm{mic}} + kT\ln(\gamma_i y_i) \tag{4}$$

Here, $\mu^0_{i,\mathrm{mon}}$ and $\mu^0_{i,\mathrm{mic}}$ are the standard chemical potentials of the amphiphilic component i in monomeric form in water and in the micelles, respectively; γ_i is the activity coefficient of component i in the micelles. The micellization constant $K_{i,\mathrm{mic}}$ is related to the work for transferring of a monomer of component i from the solution into a micelle:

$$kT\ln K_{i,\mathrm{mic}} \equiv \mu^0_{i,\mathrm{mic}} - \mu^0_{i,\mathrm{mon}} \equiv \Delta\mu^0_{\mathrm{A,mic}} \tag{5}$$

The combination of Eqs. (4) and (5) leads to [25,26]:

$$\gamma_i y_i K_{i,\mathrm{mic}} = x_i\mathrm{CMC_M} \tag{6}$$

Eq. (6) has several corollaries. First, Eq. (6) can be represented in the form:

$$\frac{\hat{c}_i}{K_{i,\mathrm{mic}}} = \gamma_i y_i \tag{7}$$

where $\hat{c}_i \equiv x_i CMC_M$ is the concentration of monomers of the respective component. Eq. (7) is a generalized form of the Raoult's law stating that the concentration of component i in monomeric form is proportional to the activity, $\gamma_i y_i$, of this component in the micelles (Fig. 4). (The conventional Raoult's law corresponds to $\gamma_i = 1$, i.e., to ideal mixing.) The form of Eq. (7) is analogous to the relationship

Table 2
Saturation ratio, $A_{sat} = c_{A,sat}/c_S$, determined from the linear regressions in Fig. 3 (T = 25 °C).

n	Saturation ratio A_{sat}	
	HZ in SLES	HZ in CAPB
10	0.43*	0.24*
12	0.352 ± 0.004	0.383 ± 0.008
14	0.192 ± 0.009	0.197 ± 0.002
16	0.097 ± 0.004	0.089 ± 0.002
18	0.05*	0.05*

* Estimated from the values of $c_{A,sat}$ at 100 mM SLES or CAPB.

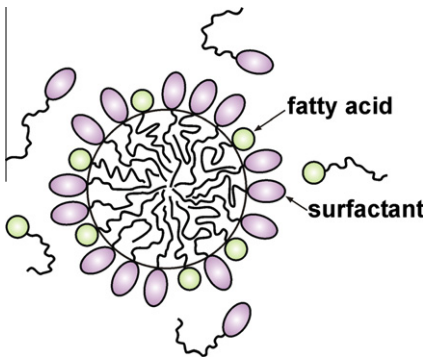

Fig. 4. Sketch of a mixed micelle composed of surfactant and fatty acid molecules, which exist in equilibrium with the free monomers in the surrounding aqueous phase.

between the molar fractions of the components in a liquid mixture, y_i, and the concentration of its vapors, $\hat{c}_i$.

Second, the summation of Eq. (6) over all amphiphilic components, in view of the relation $\sum_i x_i = 1$, leads to [25]:

$$\mathrm{CMC_M} = \sum_i \gamma_i y_i K_{i,\mathrm{mic}} \tag{8}$$

Third, Eq. (6) can be expressed in the form $\frac{y_i}{\mathrm{CMC_M}} = \frac{x_i}{\gamma_i K_{i,\mathrm{mic}}}$. Then, a summation over all amphiphilic components, along with $\sum_i y_i = 1$, yields:

$$\frac{1}{\mathrm{CMC_M}} = \sum_i \frac{x_i}{\gamma_i K_{i,\mathrm{mic}}} \tag{9}$$

For a given component, the working temperature can be *above* the Krafft temperature, T_{Krafft}, i.e., this surfactant forms micelles (rather than crystals) [27]. For a solution containing only such surfactant, the equilibrium relation between micelles and monomers acquires the form $\mu^0_{i,\mathrm{mon}} + kT \ln \mathrm{CMC}_i \equiv \mu^0_{i,\mathrm{mic}}$, where CMC_i is the critical micellization concentration of the considered surfactant [25]. The comparison of the latter equation with Eq. (5) leads to:

$$K_{i,\mathrm{mic}} = \mathrm{CMC}_i \quad \text{for} \quad T > T_{\mathrm{Krafft}} \tag{10}$$

If $T > T_{\mathrm{Krafft}}$ for all surfactants, then $K_{i,\mathrm{mic}} = \mathrm{CMC}_i$, and Eq. (9) transforms into the known expression for the CMC of mixed surfactant solutions [23,25,28–32]. In our case, however, we have to work with the more general form, Eq. (9), because at the working temperature ($T < T_{\mathrm{Krafft}}$), the fatty acids form crystallites (rather than micelles) in pure water.

In the case of ionic surfactant, such as SLES, two approaches are possible: theoretical and semiempirical. The theory of ionic–nonionic surfactant mixtures with account for the electrostatic contribution to the energy of micellization [29,33,34] can be used. This *theoretical* approach demands knowledge of the values of micelle aggregation number, N_{agg}, and charge, Z. The variations of N_{agg} and Z with the rise of surfactant concentration [35], which are related to the effects of counterion binding and Debye screening, have to be taken into account. This approach is the most reliable, but its application is related to considerable additional work, both experimental and computational.

The *semiempirical* approach to the mixed micelles of ionic and nonionic surfactants was first proposed by Mysels and Otter [26] and systematically described by Bourrel and Schechter [25]. In this approach, the theory of regular solutions is combined with two experimentally established relationships. The first one is the known fact that above the CMC, the surface tension of ionic surfactant solutions is almost constant. In view of the Gibbs adsorption equation, this means that the activity of the ionic surfactant monomers is also (almost) constant. Then, Eq. (10) can be used again, and the constant $K_{i,\mathrm{mic}}$ determined in this way to be incorporated into the theory of mixed micelles; see Eqs. (6)–(9). The second empirical relationship expresses the experimental fact that CMC_i decreases linearly with the concentration of added salt, C_{salt}, when plotted in double logarithmic scale [36]. To take into account the latter effect, the parameter $K_{i,\mathrm{mic}} = \mathrm{CMC}_i$ for the ionic surfactant is estimated from the expression [25,26]:

$$\ln \frac{\mathrm{CMC}_i}{\mathrm{CMC}_{i,0}} = -k_{\mathrm{gi}} \ln \frac{\mathrm{CMC}_i + C_{\mathrm{salt}}}{\mathrm{CMC}_{i,0}} \tag{11}$$

The subscript '0' refers to solutions without added salt. For the used sample of SLES, the experimentally determined parameters in Eq. (11) are $\mathrm{CMC}_{i,0} = 0.7$ mM and $k_{\mathrm{gi}} = 0.39$.

In the present paper, we are using the semiempirical approach in the special case without added salt.

4.2. Interpretation of the solubility limit

In our case, the micelles represent a mixture of two amphiphilic components: A – non-dissociated fatty acid and S – surfactant. (The effect of fatty acid dissociation is estimated in Appendix A; this effect turns out to be negligible at the experimental pH values; the admixtures in CAPB are treated as explained at the end of Section 3.1.) The theory of regular solutions gives the following expression for the activity coefficient of a component in a binary mixture [37]:

$$\gamma_i = \exp[\beta(1-y_i)^2], \quad \beta \equiv -\frac{cw}{2kT}, \quad i = \mathrm{A,S} \tag{12}$$

where β is the interaction parameter; c is the average number of closest neighbors of a given molecule in a micelle, and

$$w = w_{\mathrm{AA}} + w_{\mathrm{SS}} - 2w_{\mathrm{AS}} \tag{13}$$

Here, w_{ij} is the energy of interaction between two closest neighbor molecules of type i and j. As a rule, w_{ij} is negative (attraction between two neighboring molecules) [37]. In contrast, w can be negative, positive, or zero. If $w = 0$, the micellar pseudophase represents an ideal mixture of its components (neutral mixing). The cases $\beta < 0$ and $\beta > 0$ correspond to negative and positive deviations from the Raoult's law (see Eqs. (7) and (12)), i.e., to energetically favorable and unfavorable mixing of the two components in the micellar pseudophase.

The solubility limit of the fatty acids in surfactant solutions can be explained on the basis of Eq. (7) as follows: The addition of fatty acid (component A) to the solution results in increase of its mole fraction, y_{A}, in the micelles. From Eq. (7), it follows that the increase in y_{A} leads to increase in the concentration, $\hat{c}_{\mathrm{A}}$, of fatty acid monomers in the surrounding aqueous phase (Fig. 4). Precipitate of fatty acid crystallites (or droplets) appears when $\hat{c}_{\mathrm{A}}$ reaches the solubility limit for the respective fatty acid in pure water, S_{A}. Then, Eq. (7) written for $i = \mathrm{A}$ acquires the form:

$$\frac{S_{\mathrm{A}}}{K_{\mathrm{A,mic}}} = \gamma_{\mathrm{A}}(y_{\mathrm{A,sat}}) y_{\mathrm{A,sat}} \tag{14}$$

As before, $y_{\mathrm{A,sat}}$ is the value of y_{A} at saturation, and $\gamma_{\mathrm{A}} = \gamma_{\mathrm{A}}(y_{\mathrm{A,sat}})$ reflects the circumstance that the micellar activity coefficient, γ_i, depends on the micelle composition, y_i; see Eq. (12).

In view of Eqs. (12), (14) represents an implicit equation for determining $y_{\mathrm{A,sat}}$. The left-hand side of Eq. (14) is a ratio of two constants, independent of the surfactant concentration, c_{S}. Consequently, $y_{\mathrm{A,sat}}$ must be also independent of c_{S}. Thus, we conclude that $A_{\mathrm{sat}} = y_{\mathrm{A,sat}}/(1 - y_{\mathrm{A,sat}})$ must be a constant, which is in full agreement with the experimental finding that the saturation concentration grows linearly with the surfactant concentration: $c_{\mathrm{A,sat}} = A_{\mathrm{sat}} c_{\mathrm{S}}$; see Fig. 3 and Eq. (2). This result is an additional argument in favor of the proposed explanation of the solubility limit on the basis of Eq. (14).

Eq. (14) predicts that $c_{\mathrm{A,sat}}/c_{\mathrm{S}} = \text{const.}$ irrespective of the specific form of the dependence $\gamma_{\mathrm{A}}(y_{\mathrm{A,sat}})$, i.e., of whether the regular solution model, Eq. (12), or another model is used. In addition, the conclusion that $c_{\mathrm{A,sat}}/c_{\mathrm{S}} = \text{const.}$ holds irrespective of whether $\beta = 0$ or $\beta \neq 0$ in Eq. (12). Consequently, the linear dependences in Fig. 3 do not allow us to conclude whether the micelles represent an ideal or non-ideal mixture of surfactant and fatty acid.

Our next goal is to determine the fatty acid solubilization constant $K_{\mathrm{A,mic}}$ and the interaction parameter β in Eqs. (12) and (14) by means of a further analysis of the obtained experimental data. For this goal, we need the values of the fatty acid solubility in pure water, S_{A}, for the five investigated acids ($n = 10$, 12, 14, 16, and 18) at the four working temperatures ($T = 25$, 30, 35, and 40 °C).

4.3. Determination of S_A by interpolation of literature data

For $n \geqslant 10$, the fatty acid solubility in pure water, S_A, is low and difficult for experimental determination. To find S_A, we interpolated solubility data by Lucassen [16] at 20 °C and by Khuwijitjaru et al. [38] for $T \geqslant 60$ °C, see Fig. 5a. The data in Ref. [38] at the higher temperatures are obtained at higher pressures, 5 and 15 MPa, to prevent boiling. No pronounced effect of pressure on S_A was found [38].

We interpolated the data for $\log S_A$ vs. T in Fig. 5a with the linear equation:

$$\log S_A = \log S_A^{(20)} + B_n(T - 20) \tag{15}$$

where B_n is a slope coefficient depending on the number of carbon atoms in the acid chainlength, n; S_A is measured in M; T is given in °C, and $S_A^{(20)}$ is given by the expression for solubility of fatty acids at 20 °C obtained in Ref. [16]:

$$\log S_A^{(20)} = 2.82 - 0.65n \tag{16}$$

The values of the slope coefficient B_n at different n and the respective forms of Eq. (15) are given in Appendix B, Table B.1. The plot of B_n vs. n is excellently described by a straight line of equation

$$B_n = 0.00419(n - 8) + 0.00147 \tag{17}$$

(see Fig. 5b). Assuming that Eq. (17) is valid also for n = 16 and 18, we calculated the values of B_n also for palmitic and stearic acids. The results obtained at n = 16 and 18 are also given in Appendix B, Table B.1. Finally, from Eq. (15), we determined S_A for the investigated fatty acids (n = 10–18) at the four working temperatures; the results are presented in Table 3.

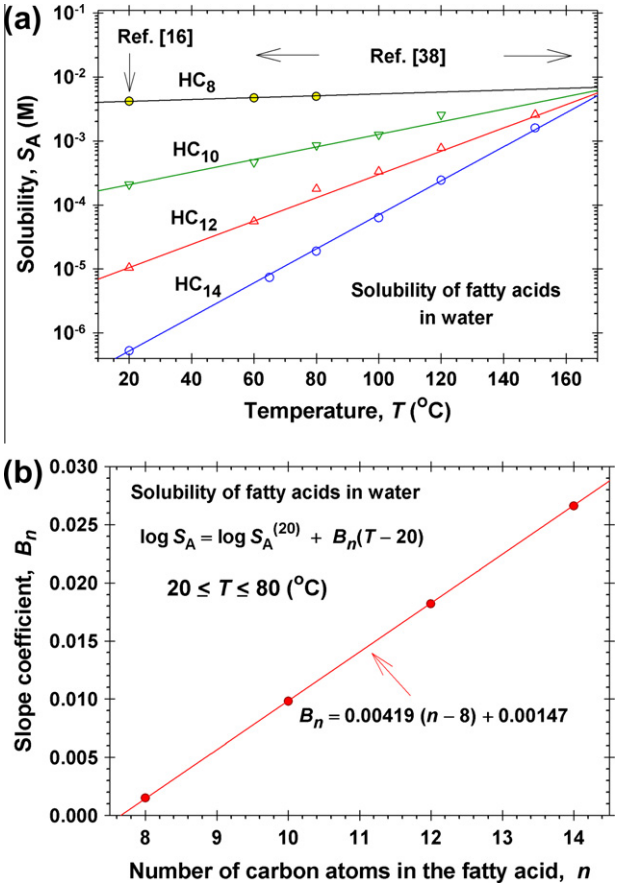

Fig. 5. (a) Plot of data for the limiting solubility of fatty acids in water, S_A, vs. the temperature, T; the data at 20 °C are from Ref. [16], whereas the data for $T \geqslant 60$ °C are from Ref. [38]. The solid lines are fits by linear regressions in accordance with Eq. (15). (b) Plot of the slopes of the lines in Fig. 5a, B_n, vs. the number of carbon atoms, n; the solid line is fit in accordance with Eq. (17); see also Table B.1 in Appendix B.

4.4. Ideal vs. non-ideal mixing of surfactant and fatty acid in the micelles

In analogy with the derivation of Eq. (5), it can be proven that $\ln S_A$ represents the energy gain from the transfer of a fatty acid molecule from a fatty acid crystal into the water phase, as a monomer:

$$kT \ln S_A \equiv \mu^0_{A,cryst} - \mu^0_{A,mon} \tag{18}$$

As demonstrated by Lucassen [16], the magnitude of this energy difference linearly increases with the chainlength, n:

$$\ln S_A = a_0 + a_1 n \tag{19}$$

where a_0 and a_1 are parameters independent of n. Similar linear dependencies hold also for carboxylates and acid soaps [16,18,20]. This fact is related to the energy for transfer of a CH_2 group from aqueous to non-aqueous environment and is physically analogous to the known Traube's rule for the adsorption of surfactants from a given homologous series [39,40]. For similar reasons, the standard energy of transfer of a fatty acid molecule from aqueous environment into the micellar pseudophase is also a linear function of the chainlength, n:

$$\ln K_{A,mic} = k_0 + k_1 n \tag{20}$$

where k_0 and k_1 are parameters that are independent of n; see Eq. (5) and Refs. [25,41]. The values of a_0 and a_1, obtained from linear fits of the data in Table 3, are given in Table 4. The values of k_0 and k_1 can be determined from the data for the solubility limits of fatty acids in surfactant micelles as explained below.

Taking logarithm of Eq. (14) and using Eqs. 12, 19, and 20, we obtain:

$$\ln(y_{A,sat}) = q_0 + q_1 n - \beta(1 - y_{A,sat})^2 \tag{21}$$

where

$$q_0 = a_0 - k_0; \quad q_1 = a_1 - k_1 \tag{22}$$

From Eq. (21), it follows that for $\beta = 0$ (ideal solution), $\ln(y_{A,sat})$ should be a linear function of the number of carbon atoms in the fatty acid molecule, n. To check this theoretical prediction, the data for $y_{A,sat}$ vs. n from Table 1 are plotted in semi-logarithmic scale in Fig. 6.

For n = 14, 16, and 18, all 8 experimental curves in Fig. 6 comply with straight lines. In view of Eq. (21), we can hypothesize that the respective mixed micelles behave as an ideal mixture ($\beta = 0$). The physical reason for this behavior can be the matching between the chainlengths of the respective acids and surfactants [31]. (Note that both CAPB and SLES are blends of molecules of different hydrocarbon chains, whose lengths vary in a certain interval that includes n = 14–18.) Setting $\beta = 0$ in Eq. (21), we obtain:

Table 3
The decimal logarithm of the solubility limit, S_A (M), for saturated fatty acids in pure water determined from experimental data [16,38] at various chainlengths, n, and temperatures.

n	$-\log S_A$ at 25 °C	$-\log S_A$ at 30 °C	$-\log S_A$ at 35 °C	$-\log S_A$ at 40 °C
10	3.63	3.58	3.53	3.48
12	4.89	4.80	4.71	4.62
14	6.15	6.01	5.88	5.75
16	7.41	7.23	7.06	6.88
18	8.66	8.45	8.23	8.01

Table 4
Values of a_0 and a_1 determined from the data in Table 3 (n = 10–18) for different temperatures.

T (°C)	$\ln S_A = a_0 + a_1 n$	
	a_0	a_1
25	6.12	−1.45
30	5.76	−1.40
35	5.39	−1.35
40	5.02	−1.30

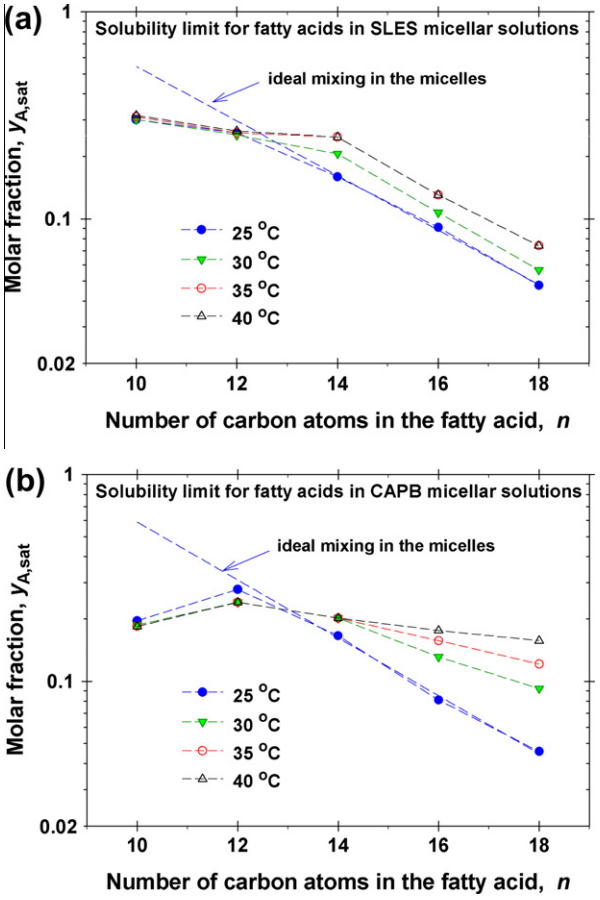

Fig. 6. The solubility limit, $y_{A,sat}$, vs. the number of carbon atoms in the paraffin chain, n, for five fatty acids (n = 10, 12, 14, 16, and 18) in (a) SLES and (b) CAPB solutions at four temperatures. In the case of ideal mixing of surfactant and fatty acid in the micelles ($\beta = 0$), the dependence $y_{A,sat}$ vs. n must be a straight line; see Eq. (21). Deviations from linearity indicate non-ideal mixing of the two components in the micelle ($\beta \neq 0$). The lines are guides to the eye.

Table 5
Values of q_0 and q_1 determined from the linear fits of the data for n = 14, 16 and 18 in Fig. 6 with Eq. (23); k_0 and k_1 are calculated from Eq. (22) and Table 4.

T (°C)	HC_n in SLES				HC_n in CAPB			
	q_0	q_1	k_0	k_1	q_0	q_1	k_0	k_1
25	2.41	−0.303	3.71	−1.15	2.69	−0.322	3.43	−1.13
30	2.95	−0.323	2.80	−1.08	1.14	−0.196	4.62	−1.20
35	2.82	−0.302	2.56	−1.05	0.211	−0.129	5.18	−1.22
40	2.82	−0.302	2.19	−0.998	−0.719	−0.0632	5.74	−1.24

$$\ln(y_{A,sat}) = q_0 + q_1 n \quad (n = 14, 16, 18) \tag{23}$$

Table 5 shows the values of q_0 and q_1, which were obtained by fitting the linear portions of the experimental curves in Fig. 6 with linear regressions in accordance with Eq. (23). Furthermore, the values of k_0, k_1, $K_{A,mic}$, and $\Delta\mu^0_{A,mic}/kT$ were calculated by using, consecutively, Eqs. 22, 20, and 5. The results are presented in Tables 5 and B.2 (the latter is in Appendix B).

For n = 10 and 12, the experimental points are located below the aforementioned linear dependences (Fig. 6). In view of Eq. (21), this can be interpreted as indication for non-ideal mixing of the surfactant and fatty acid in the micelles, i.e., $\beta \neq 0$. The physical reason for this behavior can be the mismatch between the chainlengths of the respective acids and surfactants [31]; a detailed discussion is given by the end of Section 4.5. The interaction parameter β can be estimated from the expression:

$$\beta = \frac{1}{(1 - y_{A,sat})^2} \ln\left(\frac{S_A}{y_{A,sat} K_{A,mic}}\right) \tag{24}$$

Eq. (24) follows from Eqs. (12) and (14). To calculate β, the respective values of $y_{A,sat}$, S_A, and $K_{A,mic}$ from Tables 1, 3 and B.2 have been substituted in Eq. (24). The obtained β values are given in Table 6, together with the respective values of the activity coefficient at saturation, $\gamma_{A,sat}$, calculated from Eq. (12) with $y_A = y_{A,sat}$. For n = 14, 16, and 18, the values in Table 6 indicate behavior close to ideal mixing, $\beta \approx 0$ and $\gamma_{A,sat} \approx 1$; see also Fig. 6. For n = 10 and 12, we have $\beta > 0$ (Table 6), which indicates that the energy of the system increases upon mixing of the fatty acid with the surfactant molecules in the micelles. This energy change opposes the mixing, so that in the considered case, the mixing is driven by entropy. The obtained values show that at 40 °C, the lauric acid (n = 12) also exhibits an ideal mixing ($\beta \approx 0$) in the CAPB micelles (Table 6).

4.5. Discussion

The values of the interaction parameter β in Table 6 are reasonable, having in mind that in all cases $\beta < 4$. In the regular solution theory [37], $\beta < 4$ means that the mixed micelles behave as a single pseudophase. In contrast, $\beta > 4$ would correspond to a phase separation, i.e., decomposition of the micellar pseudophase to two

Table 6
Values of the interaction parameter β and the activity coefficient $\gamma_{A,sat}$ determined from Eqs. (12) and (24), and the data in Tables 1, 3 and B.2.

n	HC_n in SLES		HC_n in CAPB	
	β	$\gamma_{A,sat}$	β	$\gamma_{A,sat}$
T = 25 °C				
10	1.189	1.789	1.701	3.005
12	0.226	1.132	0.203	1.111
14	0.004	1.003	−0.035	0.976
16	−0.049	0.961	0.058	1.050
18	0.001	1.001	−0.027	0.976
T = 30 °C				
10	1.885	2.513	1.287	2.342
12	0.800	1.561	0.351	1.22
14	0.009	1.006	−0.021	0.987
16	0.020	1.016	0.036	1.027
18	0.009	1.008	−0.016	0.987
T = 35 °C				
10	2.040	2.638	0.921	1.847
12	0.995	1.726	0.145	1.087
14	−0.025	0.986	0.004	1.003
16	0.033	1.025	−0.007	0.995
18	−0.016	0.987	0.003	1.003
T = 40 °C				
10	2.036	2.599	0.516	1.410
12	0.971	1.691	−0.096	0.946
14	−0.025	0.986	−0.006	0.996
16	0.033	1.025	0.012	1.008
18	−0.016	0.987	−0.006	0.996

coexistent phases of different composition. There are no experimental evidences for such phase separation in our case.

In Fig. 7, we compare the energy gains (in terms of standard chemical potentials) from the transfer of a fatty acid molecule between two different phases at 25 °C. First, as mentioned above, $kT\ln S_A = \mu^0_{A,cryst} - \mu^0_{A,mon}$ represents the energy gain at the transfer of a fatty acid molecule from the fatty acid crystal into pure water, as a monomer. Curve A in Fig. 7 shows that this gain is negative, which means that the considered transfer is energetically disadvantageous and it happens only owing to the rise in the entropy of mixing. In addition, the decrease of $\ln S_A$ with n means that the considered transfer becomes more unfavorable with the rise of n. The magnitude of the slope $|a_1|$, which varies between 1.30 and 1.45 kT, represents the transfer energy per CH_2 group; see Table 4 and Eq. (19). This energy is greater than the value ln3 = 1.10 kT in the Traube's rule, which gives the energy for transfer of a CH_2 group upon surfactant adsorption at the air/water interface.

Table B.2 shows that at T = 25 °C, the values of $K_{A,mic}$ for SLES and CAPB are very close, indistinguishable in log scale. For this reason, curves B and C in Fig. 7 are representative for both SLES and CAPB. Curve B in Fig. 7 represents $-\ln K_{A,mic} = (\mu^0_{A,mic} - \mu^0_{A,mon})/kT$ vs. n, which is the energy gain at the transfer of a fatty acid monomer from the water phase into a surfactant micelle. This gain is positive, which means that the considered transfer is energetically advantageous. In addition, the increase of $-\ln K_{A,mic}$ with n means that the considered transfer becomes more favorable with the rise of n. The magnitude of the slope $|k_1|$ that varies between 1.10 and 1.25 kT (see Table 5) represents the respective transfer energy per CH_2 group, which is close to the energy gain upon adsorption (the Traube's rule).

Curve C in Fig. 7 represents $(\mu^0_{A,cryst} - \mu^0_{A,mic})/kT$ vs. n, which is the energy gain at the transfer of a fatty acid monomer from a fatty acid crystal into a surfactant micelle. (Curve C is the algebraic sum of curves A and B.) This gain is slightly negative, which means that the considered transfer is energetically disadvantageous and is driven by the entropy of mixing of component A in the micelles. The negative slope of curve C means that the considered transfer becomes less favorable with the rise of n. The magnitude of the slope $|q_1|$ is in the range between 0.05 and 0.32 kT [see Table 5 and Eq. (22)]; $|q_1|$ is considerably smaller than $|a_1|$ and $|k_1|$ and expresses the transfer energy per CH_2 group between two different *non-aqueous* phases: viz. a fatty acid crystallite and the micellar pseudophase.

Fig. 8 shows plots of the solubilization energy per fatty acid molecule, $-\ln K_{A,mic}$, vs. the fatty acid chainlength, n, at different temperatures; see Table B.2. The effect of temperature is relatively weak. For the SLES solutions (Fig. 8a), the temperature effect is the greatest at n = 18, whereas for the CAPB solutions (Fig. 8b), it is the greatest at n = 10. In addition, it is interesting to note that the slope of the dependencies, $|k_1|$, which expresses the transfer energy per CH_2 group, decreases with the rise of T for SLES, but increases for CAPB (see Table 5), the effect being weak in both cases.

The fatty acid solubilization energy, $\Delta\mu^0_{A,mic} = -kT\ln K_{A,mic}$, is defined with respect to a standard state (medium), which is the micellar pseudophase from the basic surfactant, CAPB or SLES. Because CAPB represents a compound surfactant including molecules of different chainlengths, it forms an average medium where the fatty acid molecules are "dissolved". Variations in the distribution of chainlengths in different CAPB samples may, in principle, lead to variations in $K_{A,mic}$. However, the fact that $K_{A,mic}$ is practically the same for CAPB and SLES (see curve B in Fig. 7 and Table B.2) indicates that the variation in the chainlength distribution produces a minor effect. This fact complies with the model treatment of the micelle hydrophobic core as a drop of liquid hydrocarbon. In the Prigogine's molecular theory of liquid hydrocarbons [42], the paraffin chains are subdivided into elementary fragments, CH–CH and CH_3, which are treated just like separate molecules of equal volumes interacting through the Lennard-Jones potential. From this viewpoint, the variation in the chainlength distribution of CAPB (and other compound surfactants) is not expected to produce a significant effect on $K_{A,mic}$, unless it essentially affects the micellar radius.

Another issue that deserves to be discussed is the effect of carboxylate anions, Z^-, on the determined thermodynamic parameters

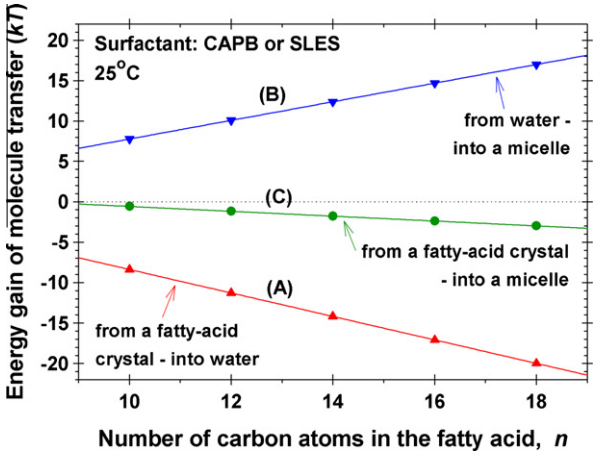

Fig. 7. Energy gain from the transfer of a fatty acid molecule: Curve A – from a fatty acid crystal into water: $\mu^0_{A,cryst} - \mu^0_{A,mon} = kT\ln S_A$; Curve B – from water into a surfactant micelle: $\mu^0_{A,mon} - \mu^0_{A,mic} = -kT\ln K_{A,mic}$, and Curve C – from a fatty acid crystal into a surfactant micelle: $\mu^0_{A,cryst} - \mu^0_{A,mic} = kT(\ln S_A - \ln K_{A,mic})$.

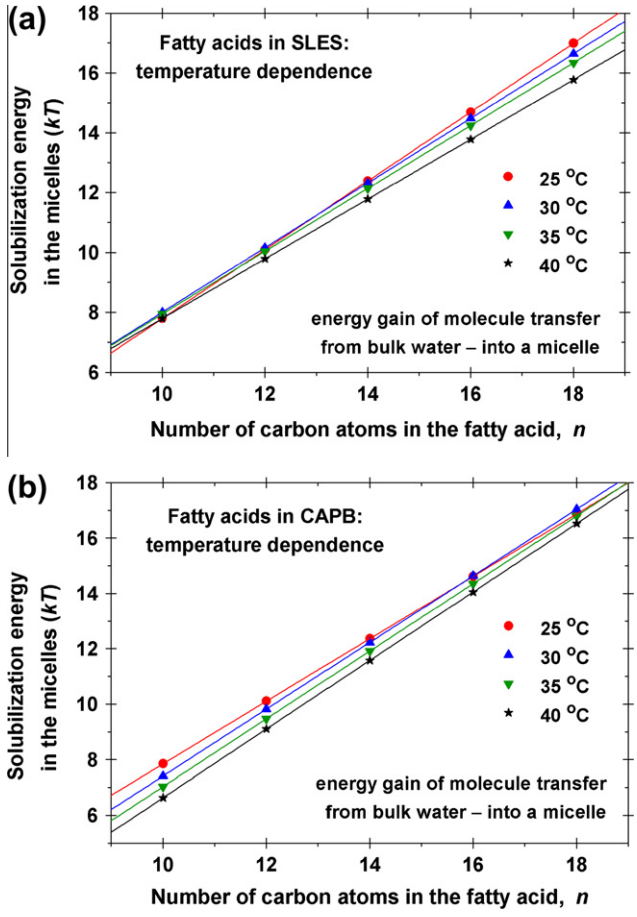

Fig. 8. Standard solubilization energy, $\Delta\mu^0_{A,mic}/(kT) = -lnK_{A,mic}$, vs. the number of carbon atoms in the fatty acid molecule, n, at various temperatures. (a) Fatty acids in SLES micelles. (b) Fatty acids in CAPB micelles.

for non-dissociated fatty acid molecules. Here, following Ref. [16], the symbol Z is used to denote carboxylate (caprate, laurate, myristate, palmitate, or stearate). If a precipitate of fatty acid crystallites is present, the dissociation–equilibrium relationship for the fatty acid reads:

$$\hat{c}_Z = \frac{K_A S_A}{c_H} \tag{25}$$

where $\hat{c}_Z$ is the concentration of Z^- monomers in the water phase; c_H is the concentration of hydrogen cations, and $K_A = 2.0 \times 10^{-5}$ M is the dissociation constant of the fatty acid. For $n \geqslant 10$, K_A is independent of n [16]. In view of Eq. (7), the activity of the carboxylate anions in the micellar pseudophase is:

$$\gamma_Z y_Z = \frac{\hat{c}_Z}{K_{Z,mic}} \tag{26}$$

In Appendix A, $\hat{c}_Z$ is determined from Eq. (25) substituting the experimental pH values at saturation ($c_A = c_{A,sat}$). Next, with literature data for $K_{Z,mic}$, we estimated $\gamma_Z y_Z$ from Eq. (26). The results (Appendix A, Table A.1) show that for all investigated carboxylic acids (n = 10–18), $\gamma_Z y_Z < 0.006$. In other words, the effective molar fraction of carboxylic anions in the mixed micelles is very low and cannot essentially affect the determined values of the thermodynamic parameters of the fatty acids, such as $y_{A,sat}$, $K_{A,mic}$, and β.

Finally, let us discuss the fact that the fatty acids with chainlengths n = 14, 16, and 18 form *ideal* mixtures with CAPB and SLES ($\beta \approx 0$), whereas those with n = 10 and 12 form *non-ideal* mixtures ($\beta > 0$); see Table 6. The average molecular formula of CAPB, which gives the molecular weight 356 g/mol, is $C_{20}H_{40}N_2O_3$. In particular, $C_{20} = C_{13}$ (an *average* paraffin chain) + C_3 (a propyl group) + C_4 (a betaine group). The propyl group is expected to be hydrophobic, so that CAPB effectively behaves as a surfactant of chainlength C_{16}. Moreover, the adsorption energy of SLES determined from fits of surface tension isotherms [43] indicates that SLES also behaves as a surfactant of chainlength C_{16}. This has been explained with the circumstance that when the number m of the oxyethylene groups in a $C_n(EO)_mSO_4Na$ molecule is small, their effect on the adsorption characteristics is quite the same as the effect of *hydrophobic* groups [44]. Thus, both CAPB and SLES effectively behave as surfactants of C_{16} tails, which is confirmed by the almost identical fatty acid solubilization energy, $\Delta\mu^0_{A,mic} = -kT\ln K_{A,mic}$, in the micelles of these two surfactants (see curve B in Fig. 7 and Table B.2). Alkyl chain mismatches normally require differences of at least four carbon atoms. Therefore, it is not surprising that the mixing with fatty acids of n = 14, 16, and 18 is ideal, whereas for n = 10 and 12, it is non-ideal, the maximum deviation from ideal mixture being observed at n = 10.

The investigated fatty acids (n = 10–18) have the same carboxylic head groups, so that their interactions in the head group region of the mixed micelles are expected to be identical at all values of n. The ideal mixing of the fatty acid with the surfactant (SLES, CAPB) at n = 14, 16, and 18 indicates that the acid–surfactant interaction is similar to the acid–acid and surfactant–surfactant interactions. More precisely, $w_{AS} \approx \frac{1}{2}(w_{AA} + w_{SS})$; see Eq. (13). The head groups of the investigated acids and surfactants are able to form transient hydrogen bonds, but it is more likely that such bonds are formed with the surrounding water molecules rather than with the neighboring head groups of the amphiphilic molecules in the micelle.

5. Phase diagrams for fatty acids in surfactant solutions

5.1. Phase domains and input parameters

Knowing the thermodynamic parameters of the system, we can construct the phase diagrams of the investigated solutions of fatty acids and surfactants at concentrations below the liquid crystal regions. As an illustration, Fig. 9 shows diagrams for lauric acid in solutions of SLES and CAPB. The way of diagram construction is described in this section.

It is convenient to create the diagram in terms of the total concentration of surface active species, $C_T = c_A + c_S$, and the total input mole fraction of the fatty acid, $z_A = c_A/(c_A + c_S)$. As usual, c_A and c_S are the total input concentrations of fatty acid and surfactant in the solution. Both C_T and z_A are known from the experiment. A dilution of the solution with pure water corresponds to a decrease of C_T at fixed z_A, i.e., to a horizontal line in the phase diagram, like the dashed line in Fig. 9a.

The phase diagram has four domains; see Fig. 9. In the "micelles" domain, the solution contains mixed micelles of components A (fatty acid) and S (surfactant), but there are no fatty acid crystallites. In the "micelles + crystals" domain, the mixed micelles coexist with fatty acid crystallites. In the domain denoted "crystals", fatty acid crystallites are present in the solution, but micelles are absent. Finally, in the "molecular solution" domain, both micelles and crystallites are absent, and the solution contains only monomers of components A and S.

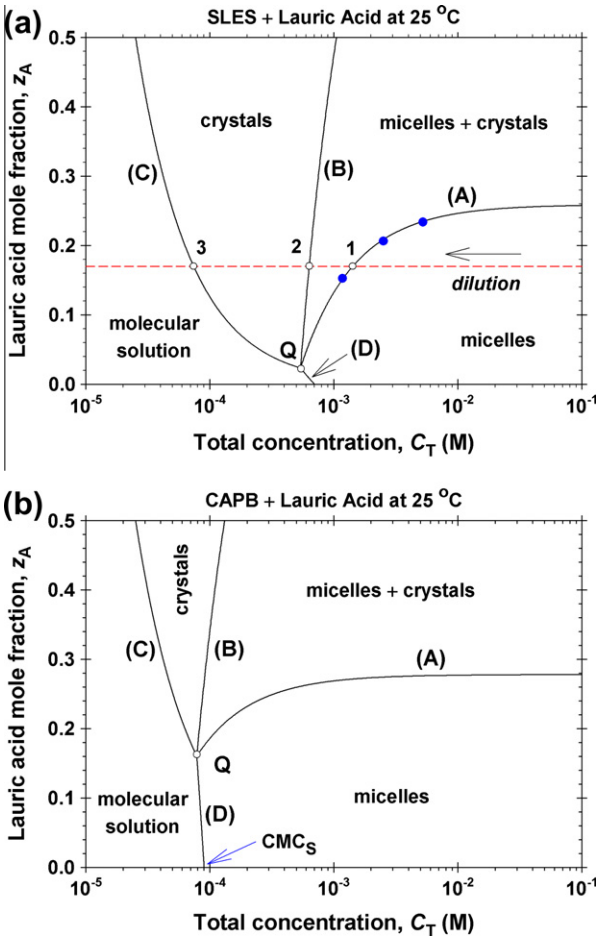

Fig. 9. Phase diagrams for solutions of surfactant and lauric acid. The solid lines A, B, C, and D represent plots of the input mole fraction of lauric acid, z_A, vs. the total concentration $c_T = c_S + c_A$ (surfactant + fatty acid) for the boundaries between the different phase domains. The notations are as follows: "micelles" = mixed micelles of surfactant and fatty acid; "crystals" = crystallites of the fatty acid; "molecular solution" = solution of monomers that contains neither micelles nor crystallites. The boundary lines intersect into a quadruple point, Q. Upon dilution (decrease of C_T at fixed z_A) the phase trajectory of the system may cross several phase domains – see the horizontal dashed line. (a) The surfactant is SLES; the three full points on the line A correspond to the kinks in Fig. 10. (b) The surfactant is CAPB.

The basic parameters of the system are S_A, $y_{A,sat}$, $K_{A,mic}$, and $K_{S,mic}$. Further, β is determined from Eq. (24). In view of Eq. (12), the activity coefficients can be calculated from the expressions:

$$\gamma_A = \exp[\beta(1-y_A)^2], \quad \gamma_S = \exp[\beta(y_A)^2] \tag{27}$$

The equations describing the inter-domain boundary lines (lines A, B, C, and D in Fig. 9) can be derived as follows.

5.2. Line A: micelles/(micelles + crystals) boundary

At this boundary, the concentration of fatty acid monomers is equal to the solubility limit, S_A, and the mole fraction of the acid in the micelles is $y_A = y_{A,sat}$. Then, in view of Eq. (8), the CMC of the mixed solution can be calculated from the expression:

$$CMC_{M,sat} = \gamma_{A,sat} y_{A,sat} K_{A,mic} + \gamma_{S,sat} y_{S,sat} K_{S,mic} \tag{28}$$

where $y_{S,sat} = 1 - y_{A,sat}$; the activity coefficients $\gamma_{A,sat}$ and $\gamma_{S,sat}$ are determined by Eq. (27) with $y_A = y_{A,sat}$.

Setting $i = A$; $y_A = y_{A,sat}$; $CMC_M = CMC_{M,sat}$; and $x_A CMC_M = S_A$ in the fatty acid mass-balance equation, Eq. (3), we obtain:

$$z_A = \left(1 - \frac{CMC_{M,sat}}{C_T}\right) y_{A,sat} + \frac{S_A}{C_T} \tag{29}$$

The $z_A(C_T)$ dependence described by Eq. (29) represents the equation of the boundary line A in Fig. 9. $CMC_{M,sat}$ is determined by Eq. (28). The line A is defined for $C_T \geqslant CMC_{M,sat}$ and ends in the quadruple point Q, whose coordinates (denoted by subscript Q) are:

$$C_{T,Q} = CMC_{M,sat}, \quad z_{A,Q} = \frac{S_A}{CMC_{M,sat}} \tag{30}$$

The expression for $z_{A,Q}$ follows from Eq. (29) at $C_T = CMC_{M,sat}$.

5.3. Line B: (micelles + crystals)/crystals boundary

At this boundary, the micelles disappear. Only fatty acid crystallites remain in the solution in the "crystals" domain. Hence, on the boundary line B the whole amount of surfactant is in the form of monomers. Then, the surfactant mass-balance equation, Eq. (3) at $i = S$, reduces to:

$$z_S C_T = x_S CMC_{M,sat} \tag{31}$$

where $CMC_{M,sat}$ is given by Eq. (28). The concentration of the fatty acid monomers is $x_A CMC_{M,sat} = S_A$ due to the presence of crystallites. Using the latter equation, along with the mole fraction relationships, $z_S = 1 - z_A$ and $x_S = 1 - x_A$, we can bring Eq. (31) in the form:

$$(1 - z_A) C_T = CMC_{M,sat} - S_A \tag{32}$$

and consequently:

$$z_A = 1 - \frac{CMC_{M,sat} - S_A}{C_T} \tag{33}$$

The $z_A(C_T)$ dependence described by Eq. (33) represents the equation of the boundary line B in Fig. 9. $CMC_{M,sat}$ is defined by Eq. (28). The line B is defined for $C_T \geqslant CMC_{M,sat}$ and ends in the quadruple point Q. Indeed, for $C_T = CMC_{M,sat}$ (the abscissa of the point Q), Eq. (33) yields $z_A = S_A/CMC_{M,sat}$ (the ordinate of the point Q); see Eq. (30). At high concentrations, $C_T \to \infty$, Eq. (33) predicts that the line B levels off at $z_A = 1$. Hence, the line B is located above the line A, which levels off at $z_A = y_{A,sat} < 1$ for $C_T \to \infty$; see Eq. (29) and Fig. 9.

5.4. Line C: crystals/(molecular solution) boundary

The "molecular solution" domain corresponds to low concentrations, at which the concentration of fatty acid monomers is smaller than the fatty acid solubility limit S_A, i.e., $z_A C_T < S_A$. Micelles are absent. At the boundary with the "crystals" region, where the first crystallites appear, we have $z_A C_T = S_A$, whence

$$z_A = \frac{S_A}{C_T} \tag{34}$$

The $z_A(C_T)$ dependence described by Eq. (34) represents the equation of the boundary line C in Fig. 9. This line is defined for $C_T \leqslant CMC_{M,sat}$ and ends in the quadruple point Q. Indeed, for $C_T = CMC_{M,sat}$ (the abscissa of the point Q), Eq. (34) yields $z_A = S_A/CMC_{M,sat}$ (the ordinate of the point Q); see Eq. (30).

5.5. Line D: (molecular solution)/micelles boundary

The line D represents the dependence of the critical micellization concentration on the composition of the mixed micelles. On this line, we have $C_T = CMC_M$, where CMC_M is given by Eq. (8). Thus, we obtain:

$$C_T(y_A) = \gamma_A y_A K_{A,mic} + \gamma_S y_S K_{S,mic} \tag{35}$$

where the activity coefficients $\gamma_A(y_A)$ and $\gamma_S(y_A)$ are given by Eq. (27). In addition, the substitution $i = A$, $C_T = CMC_M$, and $x_A CMC_M c_A = \gamma_A y A K_{A,mic}$ (see Eq. (7)), in the mass-balance equation, Eq. (3), leads to:

$$z_A C_T = \gamma_A y_A K_{A,mic} \tag{36}$$

which can be represented in the form:

$$z_A(y_A) = \frac{\gamma_A y_A K_{A,mic}}{C_T(y_A)} \tag{37}$$

Eqs. (35) and (37) describe the dependence $z_A(C_T)$ for the boundary line D in a parametric form, viz. $C_T = C_T(y_A)$ and $z_A = z_A(y_A)$, where $0 \leqslant y_A \leqslant y_{A,sat}$. At the lower limit, $y_A = 0$, Eq. (35) yields

Table 7
Coordinates of the quadruple point, Q, calculated from Eq. (30).

n	SLES		CAPB	
	$C_{T,Q}$ (M)	$z_{A,Q}$	$C_{T,Q}$ (M)	$z_{A,Q}$
10	7.81×10^{-4}	0.299	3.11×10^{-4}	0.752
12	5.39×10^{-4}	2.34×10^{-2}	7.91×10^{-5}	0.163
14	5.89×10^{-4}	1.21×10^{-3}	7.59×10^{-5}	9.39×10^{-3}
16	6.36×10^{-4}	6.19×10^{-5}	8.28×10^{-5}	4.75×10^{-4}
18	6.67×10^{-4}	3.26×10^{-6}	8.59×10^{-5}	2.53×10^{-5}

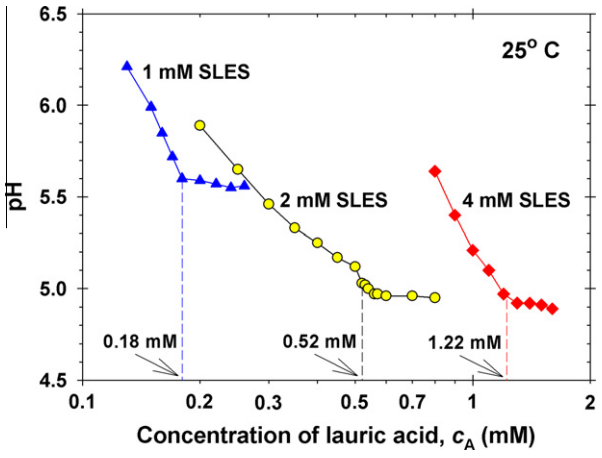

Fig. 10. Plot of experimental data for pH vs. the concentration of lauric acid, c_A. Each curve corresponds to a fixed surfactant concentration: $c_S = 1$, 2 and 4 mM SLES. The kinks of the three curves correspond to the full points in Fig. 9a, i.e. to the appearance of lauric acid crystallites.

Table A.1
Monomer concentration, $\hat{c}_Z$, and effective molar fraction, $\gamma_Z y_Z$, of the carboxylate anions in the mixed micelles of fatty acid with SLES and CAPB estimated from the experimental pH at $c_A = c_{A,sat}$; $T = 25$ °C (details in the text).

n	CMC_Z (M)	SLES			CAPB		
		pH	$\hat{c}_Z(M)$	$\gamma_Z y_Z$	pH	$\hat{c}_Z(M)$(M)	$\gamma_Z y_Z$
10	9.32×10^{-2}	5.07	5.49×10^{-4}	5.89×10^{-3}	4.90	3.71×10^{-4}	3.98×10^{-3}
12	2.26×10^{-2}	5.63	1.10×10^{-4}	4.86×10^{-3}	4.92	2.14×10^{-5}	9.47×10^{-4}
14	5.50×10^{-3}	5.92	1.18×10^{-5}	2.15×10^{-3}	4.99	1.39×10^{-6}	2.53×10^{-4}
16	1.34×10^{-3}	6.08	9.44×10^{-7}	7.07×10^{-4}	5.15	1.11×10^{-7}	8.30×10^{-5}
18	3.24×10^{-4}	6.35	9.70×10^{-8}	2.99×10^{-4}	5.18	6.56×10^{-9}	2.02×10^{-5}

Table B.1
The slope coefficient, B_n, and the form of Eq. (15) for fatty acids with n carbon atoms.

n	B_n	Eq. (15)*
8	0.0015 ± 0.001	$\log S_A = -2.38 + 0.0015(T - 20)$
10	0.0098 ± 0.0006	$\log S_A = -3.68 + 0.0098(T - 20)$
12	0.0182 ± 0.0007	$\log S_A = -4.98 + 0.0182(T - 20)$
14	0.0266 ± 0.0007	$\log S_A = -6.28 + 0.0266(T - 20)$
Predicted values assuming that Eq. (17) is valid for $n = 16$ and 18		
16	0.0350	$\log S_A = -7.58 + 0.0350(T - 20)$
18	0.0434	$\log S_A = -8.88 + 0.0434(T - 20)$

* The temperature T is measured in °C.

$C_T = K_{S,mic} = CMC_S$, which is the CMC of the surfactant solution without added fatty acid. In the upper limit, $y_A = y_{A,sat}$, in view of Eq. (28), we obtain that Eq. (35) reduces to $C_T = CMC_{M,sat} = C_{T,Q}$, and Eq. (37) yields $z_A = S_A/CMC_{M,sat} = z_{A,Q}$, which are the coordinates of the point Q; see Eq. (30). In other words, the line D also ends in the quadruple point.

5.6. Numerical results and discussion

The phase diagrams in Fig. 9 and the numerical data in Table 7 were obtained by using the following parameter values, all of them corresponding to $T = 25$ °C. The values of $y_{A,sat}$, S_A and $K_{A,mic}$ were taken from Tables 1, 3 and B.2. Next, β was calculated from Eq. (24). $K_{S,mic}$ was set equal to the surfactant's CMC, viz. $K_{S,mic} = 0.70$ and 0.09 mM for SLES and CAPB, respectively.

The coordinates of the quadruple point, $C_{T,Q}$ and $z_{A,Q}$, calculated from Eq. (30) for $n = 10$–18 are given in Table 7. As seen, $z_{A,Q}$ is systematically smaller for SLES than for CAPB, so that the quadruple point Q is located lower in the phase diagram for SLES in comparison with that for CAPB. (Compare Fig. 9a and b, which correspond to the special case $n = 12$.)

In addition, the data in Table 7 show that the abscissa of the quadruple point, $C_{T,Q}$, is close to the CMC of the respective surfactant (with an exclusion for capric acid in CAPB). As a consequence, the variation of C_T along the line D is relatively small; see e.g. Fig. 9. Having in mind that $C_T = CMC_M$ along the line D, this means that the effect of the addition of fatty acid on the solution's CMC is relatively small, in the framework of the experimental accuracy of CMC determination. For this reason, the conventional approach by Rubingh [23] and Rosen and Hua [41,45] for determining the interaction parameter β based on the effect of the additive on the solution's CMC is difficult for application in the considered cases.

The phase diagrams can predict the changes that occur upon dilution of the investigated solutions. This is illustrated by the horizontal dashed line in Fig. 9a. As mentioned above, the dilution is equivalent to decreasing of C_T at a fixed z_A. In particular, $z_A = 0.17$ for the dashed line in Fig. 9a, which intersects three of the boundary lines, A, B, and C. The respective intersection points are denoted by 1, 2 and 3. To the right of the point 1, in the domain with mixed micelles the solutions are clear. Upon dilution, the first crystallites appear at the point 1. Upon further dilution, at the point 2 the micelles disappear, but the crystallites of fatty acid are still present. At the point 3, the crystallites also disappear.

At higher surfactant concentrations, the appearance of large non-spherical micelles and liquid-crystal phases are expected, but this concentration region is out of the scope of the present study.

6. Experimental verification of the phase diagram

To verify the phase diagram, we prepared a series of solutions corresponding to a fixed concentration of SLES, c_S, and to increasing concentrations of lauric acid, c_A. At the lower values of c_A, the point (C_T, z_A) belongs to the domain "micelles" in Fig. 9a. However, at a sufficiently large c_A, the boundary line A will be crossed, so that lauric acid crystallites will appear in the solution. With this experiment, our goal is to verify whether the position of the boundary line A near the quadruple point, Q, is correctly predicted by the theory from Section 5.

Table B.2
Solubilization constant, $K_{A,mic}$, and standard solubilization energy, $-\Delta\mu^0_{A,mic}/kT$, for fatty acids at various temperatures in SLES and CAPB micelles.

n	25 °C		30 °C		35 °C		40 °C	
	$\log K_{A,mic}$	$-\frac{\Delta\mu^0_{A,mic}}{kT}$	$\log K_{A,mic}$	$-\frac{\Delta\mu^0_{A,mic}}{kT}$	$\log K_{A,mic}$	$-\frac{\Delta\mu^0_{A,mic}}{kT}$	$\log K_{A,mic}$	$-\frac{\Delta\mu^0_{A,mic}}{kT}$
SLES								
10	−3.37	7.76	−3.46	7.96	−3.44	7.91	−3.38	7.78
12	−4.37	10.1	−4.39	10.1	−4.35	10.0	−4.25	9.78
14	−5.36	12.3	−5.33	12.3	−5.26	12.1	−5.11	11.8
16	−6.36	14.6	−6.26	14.4	−6.17	14.2	−5.98	13.8
18	−7.36	16.9	−7.20	16.6	−7.08	16.3	−6.85	15.8
CAPB								
10	−3.41	7.85	−3.22	7.41	−3.05	7.03	−2.88	6.63
12	−4.39	10.1	−4.27	9.82	−4.11	9.47	−3.95	9.10
14	−5.37	12.4	−5.31	12.2	−5.17	11.9	−5.03	11.6
16	−6.35	14.6	−6.36	14.6	−6.23	14.4	−6.10	14.1
18	−7.33	16.9	−7.40	17.0	−7.30	16.8	−7.18	16.5

In the considered concentration region, the amount of fatty acid crystallites is too low, and it is impossible to be determined by measurements of absorbance (by spectrophotometer) or by an apparatus for static and dynamic light scattering. Fortunately, the pH measurements are sensitive to the appearance of fatty acid crystallites; see e.g. Ref. [18]. Fig. 10 shows plots of experimental data for pH vs. c_A for three different fixed concentrations of SLES: c_S = 1, 2, and 4 mM. Each experimental curve exhibits a kink. For each kink, we calculated $C_T = c_A + c_S$ and $z_A = c_A/C_T$, and the obtained (C_T, z_A) point is shown in Fig. 9a by a full circle. As seen, the tree points that correspond to the kinks of the three experimental curves in Fig. 10 are really lying on the curve A, i.e., on the boundary between the "micelles" and "micelles + crystals" domains in Fig. 9a. This result confirms the validity of the respective phase diagram theoretically predicted from the values of the parameters S_A, $y_{A,sat}$, $K_{A,mic}$, and $K_{S,mic}$ – see Section 5.

7. Conclusions

For the first time, a quantitative theoretical interpretation of the solubility limit of fatty acids (and other amphiphiles of limited solubility) in micellar solutions of water-soluble surfactants is presented and a general picture of the phase behavior of the investigated systems is given in the form of originally constructed phase diagrams. The limited solubility of the fatty acids in the micelles of conventional surfactants is explained with the precipitation of fatty acid monomers in the bulk, rather than with phase separation in the mixed micelles. A completely new and original approach to the determination of the parameter of interaction between the components in the mixed micelles β is developed, which is based on analysis of the dependence of the saturation concentration on the fatty acid chainlength. This approach is alternative to the known method by Rubingh [23] and Rosen [41] that is based on the dependence of CMC on the surfactant molar fractions in mixed solutions. Although the latter method works well for soluble surfactants of relatively high purity, it is not applicable to surfactant mixtures of low CMC that exhibit very slow adsorption kinetics, which is affected by minor impurities, so that the equilibrium values obtained by extrapolation are uncertain. In contrast, the proposed new approach is applicable at concentrations much above the CMC, where the micellar kinetics is fast. In this approach, to characterize the interactions between the components in the mixed micelles, it is not necessary to work at very low concentrations, at which the first micelles appear. The new approach is applicable also to compound surfactants, such as CAPB, which contain components of different chainlength, and which are currently used in practical applications. It is interesting that the long-chain fatty acids (n = 14, 16 and 18) exhibit ideal mixing in the SLES and CAPB micelles. Deviations from ideality are observed for the fatty acids of shorter chain (n = 10 and 12). The latter fact is in agreement with the observations of non-ideal behavior in ternary micellar systems containing CAPB, anionic surfactant, and a fatty acid of shorter chain [46].

Furthermore, using the values of the thermodynamic parameters of the system, its phase diagram, presenting the overall phase behavior of the system, has been constructed. Such a diagram consists of four domains, viz. mixed micelles; coexistent micelles and crystallites; crystallites without micelles; and molecular solution. Equations of the boundary lines separating these phase domains are derived. Interestingly, the four boundary lines intersect in a quadruple point, Q, whose coordinates have been obtained for the investigated systems. The results may contribute to understanding, quantitative interpretation and prediction of the phase behavior of mixed micellar solutions that contain a water-soluble surfactant and an amphiphile of limited solubility, such as fatty acid, fatty alcohol, sodium carboxylate, glycinate, etc.

Acknowledgments

We thankfully acknowledge the support from Unilever R&D, Trumbull, USA, and from the National Science Fund of Bulgaria, Grant No. DCVP 02/2-2009, UNION.

Appendix A. Estimation of the mole fraction of carboxylate anions in the mixed micelles

The following values of the critical micellization concentration of sodium carboxylates, CMC_Z, have been determined at 25 °C: for n = 8, CMC_Z = 0.390 M [47]; for n = 10, CMC_Z = 0.090 M [48], and for n = 12, CMC_Z = 0.023 M [49]. The plot of these data as log CMC_Z vs. n complies with a straight line of equation:

$$\log \mathrm{CMC}_Z = 2.0424 - 0.3073\, n \tag{A.1}$$

The squared correlation coefficient of the fit with Eq. (A.1) is R^2 = 0.9996. Linear dependencies, like that in Eq. (A.1), are known for homolog series of many surfactants [25,41]. All CMC_Z values in Table A.1 are estimated from Eq. (A.1).

In our experiments, we measured the natural pH of the investigated mixed solutions of fatty acid and surfactant at the saturation point, at which $c_A = c_{A,sat}$. The obtained pH values are given in Table A.1 for SLES and CAPB. Next, using Eq. (25) and the data for S_A from Table 3, we estimated the concentration $\hat{c}_Z$ of the free carboxylate anions in the solution. Finally, substituting $\hat{c}_Z$ in Eq. (26) with $K_{Z,mic} = CMC_Z$, we calculated the effective mole fraction, $\gamma_Z y_Z$, of the carboxylate anions (Z^-) that are incorporated into micelles. The obtained values of $\hat{c}_Z$ and $\gamma_Z y_Z$ are also given in Table A.1.

The obtained values of $\gamma_Z y_Z$ at saturation are by orders of magnitude smaller than the values of $y_{A,sat}$ for the same n in Table 1 (note that the activity coefficient γ_Z is on the order of (1). Hence, only a very small fraction of the input amount of fatty acid dissociates to Z^- and H^+ ions. Therefore, the use of the total input fatty acid concentration, $c_{A,sat}$, in Eq. (1) gives a correct estimate of the fatty acid mole fraction at saturation, $y_{A,sat}$.

Appendix B. Tabulated thermodynamic parameters

Table B.1 contains data for the temperature dependence of the solubility of fatty acids in pure water obtained as explained in Section 4.3. Table B.2 summarizes the determined solubilization constants and standard solubilization energies for fatty acids of chainlength n in micellar solutions of SLES and CAPB.

References

[1] K. Mysels, K. Shinoda, S. Frankel, Soap Films, Pergamon, London, 1959.
[2] D.A. Edwards, H. Brenner, D.T. Wasan, Interfacial Transport Processes and Rheology, Butterworth-Heinemann, Boston, 1991.
[3] I.B. Ivanov, K.D. Danov, P.A. Kralchevsky, Colloids Surf. A 152 (1999) 161.
[4] S.A. Koehler, S. Hilgenfeldt, H.A. Stone, Langmuir 16 (2000) 6327.
[5] K. Golemanov, S. Tcholakova, N.D. Denkov, K.P. Ananthapadmanabhan, A. Lips, Phys. Rev. E 78 (2008) 051405.
[6] K. Tsujii, Surface Activity: Principles, Phenomena and Applications, Academic Press, London, 1998.
[7] W. Xu, A. Nikolov, D.T. Wasan, A. Gonsalves, R.P. Borwankar, Colloids Surf. A 214 (2003) 13.
[8] A. Saint-Jalmes, D. Langevin, J. Phys.: Condens. Matter 14 (2002) 9397.
[9] O. Pitois, C. Fritz, M. Vignes-Adler, J. Colloid Interface Sci. 282 (2005) 458.
[10] O. Pitois, C. Fritz, M. Vignes-Adler, Colloids Surf. A 261 (2005) 109.
[11] N.D. Denkov, V. Subraminian, D. Gurovich, A. Lips, Colloids Surf. A 263 (2005) 129.
[12] K. Golemanov, N.D. Denkov, S. Tcholakova, M. Vethamuthu, A. Lips, Langmuir 24 (2008) 9956.
[13] B. Dollet, J. Rheol. 54 (2010) 741.
[14] N.D. Denkov, S. Tcholakova, K. Golemanov, V. Subramanian, A. Lips, Colloids Surf. A 282 (2006) 329.
[15] N.D. Denkov, S. Tcholakova, K. Golemanov, K.P. Ananthpadmanabhan, A. Lips, Soft Matter 5 (2009) 3389.
[16] J. Lucassen, J. Phys. Chem. 70 (1966) 1824.

[17] X. Wen, E.I. Franses, J. Colloid Interface Sci. 231 (2000) 42.
[18] P.A. Kralchevsky, K.D. Danov, S.D. Kralchevska, C.I. Pishmanova, N.C. Christov, K.P. Ananthapadmanabhan, A. Lips, Langmuir 23 (2007) 3538.
[19] P.A. Kralchevsky, M.P. Boneva, K.D. Danov, K.P. Ananthapadmanabhan, A. Lips, J. Colloid Interface Sci. 327 (2008) 169.
[20] M.P. Boneva, K.D. Danov, P.A. Kralchevsky, S.D. Kralchevska, K.P. Ananthapadmanabhan, A. Lips, Colloids Surf. A 354 (2010) 172.
[21] S. Soontravanich, H.E. Lopez, J.F. Scamehorn, D.A. Sabatini, D.R. Scheuing, J. Surfactants Deterg. 13 (2010) 367.
[22] S. Soontravanich, J.G. Landrum, S.A. Shobe, C.M. Waite, J.F. Scamehorn, D.A. Sabatini, D.R. Scheuing, J. Surfactants Deterg. 13 (2010) 373.
[23] D.N. Rubingh, in: K.L. Mittal (Ed.), Solution Chemistry of Surfactants, vol. 1, Plenum Press, New York, 1979, p. 337.
[24] G. Knothe, R.O. Dunn, J. Am. Oil Chem. Soc. 86 (2009) 843.
[25] M. Bourrel, R.S. Schechter, Microemulsions and Related Systems, M. Dekker, New York, 1988. p. 87.
[26] K.J. Mysels, R.J. Otter, J. Colloid Sci. 16 (1961) 474.
[27] C.H. Rodriguez, J.F. Scamehorn, J. Surfactants Deterg. 2 (1999) 17.
[28] J.H. Clint, J. Chem. Soc., Faraday Trans. 1 (71) (1975) 1327.
[29] M. Bergstrom, P. Jonsson, M. Persson, J.C. Eriksson, Langmuir 19 (2003) 10719.
[30] S. Paria, Colloids Surf. A 281 (2006) 113.
[31] P.C. Schulz, J.L. Rodriguez, R.M. Minardi, M.B. Sierra, M.A. Morini, J. Colloid Interface Sci. 303 (2006) 264.
[32] P. Letellier, A. Mayaffre, M. Turmine, J. Colloid Interface Sci. 354 (2011) 248.
[33] J.C. Eriksson, L.M. Bergström, M. Persson, Russ. J. Phys. Chem. 77 (2003) S87. <http://urn.kb.se/resolve?urn=urn:nbn:se:kth:diva-22701>.
[34] L.M. Bergström, M. Aratono, Soft Matter 7 (2011) 8870.
[35] B.L. Bales, M. Almgren, J. Phys. Chem. 99 (1995) 15153.
[36] M.L. Corrin, W.D. Harkins, J. Am. Chem. Soc. 69 (1947) 683.
[37] T.L. Hill, An Introduction to Statistical Thermodynamics, Dover, New York, 1987.
[38] P. Khuwijitjaru, S. Adachi, R. Matsuno, Biosci. Biotechnol. Biochem. 66 (2002) 1723.
[39] A.W. Adamson, Physical Chemistry of Surfaces, 4th ed., Wiley, New York, 1982. p. 92.
[40] K.D. Danov, P.A. Kralchevsky, K.P. Ananthapadmanabhan, A. Lips, J. Colloid Interface Sci. 300 (2006) 809.
[41] M.J. Rosen, Surfactants and Interfacial Phenomena, Wiley, New York, 2004. p. 381.
[42] I. Prigogine, The Molecular Theory of Solutions, North Holland Publishing Co., Amsterdam, 1957. p. 338.
[43] D. Vollhardt, G. Czichocki, R. Rudert, Colloids Surf. A 142 (1998) 315.
[44] V.B. Fainerman, R. Miller, E.V. Aksenenko, A.V. Makievski, in: V.B. Fainerman, D. Möbius, R. Miller (Eds.), Surfactants: Chemistry, Interfacial Properties, Applications, Elsevier, Amsterdam, 2001, p. 242 (Chapter 3).
[45] X.Y. Hua, M.J. Rosen, J. Colloid Interface Sci. 90 (1982) 212.
[46] G. Colafemmina, R. Recchia, A.S. Ferrante, S. Amin, G. Palazzo, J. Phys. Chem. B 114 (2010) 7250.
[47] B. Lindman, B. Brun, J. Colloid Interface Sci. 42 (1973) 388.
[48] K. Morigaki, P. Walde, M. Misran, B.H. Robinson, Colloids Surf. A 213 (2003) 37.
[49] K.A. Coltharp, E.I. Franses, Colloids Surf. A 108 (1996) 225.